Neuropathology and Applied Neurobiology (2014), **40**, 177–190 doi: 10.1111/nan.12087

A comparative study of the dentate gyrus in hippocampal sclerosis in epilepsy and dementia

R. Bandopadhyay, J. Y. W. Liu, S. M. Sisodiya and M. Thom

Department of Clinical and Experimental Epilepsy, UCL, Institute of Neurology and National Hospital for Neurology and Neurosurgery, London, UK

R. Bandopadhyay, J. Y. W. Liu, S. M. Sisodiya and M. Thom (2014) *Neuropathology and Applied Neurobiology* **40**, 177–190

A comparative study of the dentate gyrus in hippocampal sclerosis in epilepsy and dementia

Aims: Hippocampal sclerosis (HS) is long-recognized in association with epilepsy (HS_E) and more recently in the context of cognitive decline or dementia in the elderly (HS_D), in some cases as a component of neurodegenerative diseases, including Alzheimer's disease (AD) and frontotemporal lobe dementia (FTLD). There is an increased risk of seizures in AD and spontaneous epileptiform discharges in the dentate gyrus of transgenic AD models; epilepsy can be associated with an age-accelerated increase in AD-type pathology and cognitive decline. The convergence between these disease processes could be related to hippocampal pathology. HS_E typically shows re-organization of both excitatory and inhibitory neuronal networks in the dentate gyrus, and is considered to be relevant to hippocampal excitability. We sought to compare the pathology of HS_E and HS_D, focusing on re-organization in the dentate gyrus. **Methods:** In nine *post mortem* cases with HS_E and bilateral damage, 18 HS_D and 11 controls we carried out immunostaining for mossy fibres (dynorphin), and interneuronal networks (NPY, calbindin and calretinin) on sections from the mid-hippocampal body. Fibre sprouting (FS) or loss of expression in the dentate gyrus was semi-quantitatively graded from grade 0 (normal) to grade 3 (marked alteration). **Results:** Significantly more re-organization was seen with all four markers in the HS_E than HS_D group ($P < 0.01$). Mild alterations were noted in HS_D group with dynorphin (FS in 3 cases), calretinin (FS in 6 cases), NPY (FS in 11 cases) and calbindin (loss in 10 cases). In eight HS_D cases, alteration was seen with more than one antibody but in no cases were the highest grades seen. We also noted NPY and, to a lesser extent, calretinin labelling of Hirano bodies in CA1 of AD cases and some older controls, but not in HS_E. **Conclusion:** Reorganization of excitatory and inhibitory networks in the dentate gyrus is more typical of HS_E. Subtle alterations in HS_D may be a result of increased hippocampal excitability, including unrecognized seizure activity. An unexpected finding was the identification of NPY-positive Hirano bodies in HS_D but not HS_E, which may be a consequence of the relative vulnerabilities of interneurons in these conditions.

Keywords: dementia, dentate gyrus, epilepsy, hippocampal sclerosis, Hirano bodies, synaptic reorganization

Introduction

Hippocampal sclerosis (HS) is a pathological change long-associated with epilepsy and although not specific for syndrome or seizure-type, is particularly associated with mesial temporal lobe epilepsy (TLE) [1] from benign [2] to drug-resistant types. Evidence suggests it is a relatively common pathology, identified in 25% of all TLE patients on MRI [3] and histologically confirmed in 33.6% and 30–40% of surgical [1] and *post mortem* (PM) epilepsy cases [4,5] respectively. The pathological alterations of HS in epilepsy (HS_E) are well described [6], with consistent

Correspondence: Maria Thom, Department of Neuropathology, UCL, Institute of Neurology, Queen Square, London WC1N 3BG, UK. Tel: +44 020 3448 4233; Fax: +44 020 3448 4486; E-mail: M.Thom@ucl.ac.uk

patterns of neuronal loss and gliosis centred on the CA1 subfield, with more variable loss from CA4 and other subfields. More recently, the associated pathology involving the dentate gyrus has been better characterized with dispersion of the granule cell layer (GCD) [7] and sprouting of the mossy fibre axons [8] noted as common alterations. In addition to loss of principal neurones, stereotypical changes to hippocampal interneurons are well documented in surgical series, particularly in the dentate gyrus, including loss and fibre sprouting [9–13]. These alterations to the dentate gyrus, which tend to occur synchronously, are likely influenced by hippocampal seizures and excitability rather than neuronal loss and they have been observed in PM as well as surgical series of patients, where they may be bilateral [14].

HS has also been increasingly recognized on imaging and at PM in older and elderly patients, typically in the absence of a seizure history, but in association with memory impairment or dementia (HS_D). The proposed causes of HS_D are heterogenous, and include anoxic-ischaemic injury and neurodegenerative causes [15,16]. HS_D has recently been linked to TDP-43 associated pathology [17] in support of underlying degenerative mechanisms. The prevalence of HS_D in non-epilepsy, elderly PM series is around 16% [18] and is bilateral in half of the cases [16]. The pathological differences between HS_E and HS_D have not been directly compared, in particular if similar alterations in the dentate gyrus occur. Differences between HS_E and HS_D would be useful in histopathological evaluation, and may identify distinct mechanisms of cell degeneration, and alterations specific to symptoms, including seizures *vs.* memory loss. The aim of the current study was to compare the dentate gyrus pathology in a series of HS_E with HS_D PM cases, in particular with regard to the patterns of GCD, mossy fibre sprouting and interneuronal alterations.

Materials and methods

Cases were selected from the PM archives at the National Hospital for Neurology and Neurosurgery, Queen Square and from the Queen Square Brain Bank, Institute of Neurology, London (details of all cases are available in a supplemental file, Table S1). This study has been approved by the Joint Research Ethics Committee of the Institute of Neurology and appropriate consent was obtained from the patient's next of kin. We selected nine cases with bilateral hippocampal sclerosis, as confirmed at PM, from patients with epilepsy (HS_E). Four patients were male and the average age of onset of epilepsy was 11 years with mean duration of disease of 53 years, and the average age of death was 62 years (range 27–87 years). All the patients had partial epilepsy syndromes, with a diagnosis of TLE in four. We selected cases with low Braak stages [5], which included six cases with stage 1 or 2, and three with stage 3. All the patients were residents at the National Society for Epilepsy, Chalfont Centre, UK. For five patients, there was a history of progressive cognitive decline reported in later life [5].

We selected 10 cases of patients with Alzheimer's disease (AD) and diagnosis of HS_D, defined as pyramidal cells loss in the hippocampal formation that is out of proportion to the AD neuropathological changes [19]. Seven patients were male and the average age of death was 69 years (range 66–78 years). Nine cases were Braak stage 6 and one case Braak stage 5. In addition, we included eight cases with fronto-temporal lobe dementia (FTLD) and a diagnosis of HS_D, which included four males. The average age at death was 72 years (range 67–78 years) and the diagnosis was FTLD-TDP type C in three cases, type B in one case, type A in two cases, Pick's disease in one case and unspecified in one case [20]. In only one patient with AD was there a history of seizure events following onset of dementia, and in no case was epilepsy documented early in life. In addition, 11 control cases were selected with no history of AD or epilepsy; four were male and the mean age was 55 years (range 36–68 years).

In all cases, one hemisphere was selected and a block taken from the hippocampal body at the level best representing the HS pathology as evaluated on H&E and cresyl violet/luxol fast blue preparations. Sections were cut at 7 μm thickness (and 14 μm for dynorphin labelling) for immunohistochemistry. In brief, endogenous peroxidase activity was blocked with 3% hydrogen peroxide (VWR International, Pennsylvania, USA), sections were microwaved for 15 min in antigen retrieval masking buffer (Vector, Burlingame, CA, USA) and washed in phosphate buffered saline (PBS, Oxiod, Hampshire, UK). The primary antibodies, anti-neuropeptide Y (NPY, 1:4000; Sigma, USA), anti-calretinin (1:4000; Swant, Switzerland), anti-calbindin (1:10 000; Swant), anti-dynorphin (1:50; AbD Serotec, UK), GFAP (1:1500; Dako, Cambridge, UK) and GFAP-δ (1:5000; Chemicon International, Temecula, CA, USA) were diluted in Dako antibody diluent (Dako, Glostrup, Denmark) and applied overnight. DAKO envision horse radish peroxidase (HRP, Dako) was used

to detect labelling. Nuclei were counterstained with Haematoxylin (VWR International). The catalysed signal amplification was employed for the dynorphin staining (see Liu *et al*. [21] for detailed protocol).

In addition, double labelling was performed on selected HS_D cases to further characterize NPY-immunopositive Hirano bodies. In brief, sections were initially incubated overnight with anti-MAP2 (1:750; Sigma), AT8 (1:1200; Autogen Bioclear, UK), or SMI 31 (1:1000; Sternberger Monoclonal Incorporation, USA) antibodies. On the following day, Dako Envision EnVision™ HRP solution was applied for 30 min before fluorescein-labelled antibody in tyramide signal amplification (TSA) buffer (1:500; Perkin Elmer, UK) was applied for 8 min. The TSA system is a sensitive detection system that has been used in previous studies on PM human tissue [22,23]. Sections were thoroughly washed before anti-NPY antibodies (1:4000) were applied overnight. Rhodamine-labelled antibody in TSA buffer (1:500; Perkin Elmer) was incubated on sections for 8 min at room temperature, before sections were coverslipped in DAPI-mounting media (Vector). Immunofluorescent-labelled sections were viewed under a confocal laser scanning microscope (Zeiss LSM 710) equipped with blue diode, argon and helium/neon lasers.

Qualitative assessment

In each case, the degree of hippocampal neuronal loss in CA4 and CA1 and the pattern of granule cell dispersion were assessed on the H&E section and graded (Table 1) in addition to the distribution of astrocytic gliosis on GFAP and delta-GFAP sections. The presence of mossy fibre sprouting (MFS) and the expression patterns of calbindin, calretinin and NPY in the dentate gyrus (in particular loss of neuronal expression and abnormal fibre sprouting) were assessed and graded as previously described and validated in studies of HS_E (Table 1) [12–14,23]. The grading was carried out independently by two observers with good agreement (kappa scores between 0.65 and 0.74 for the four markers), and agreement reached on all cases following a joint review.

Quantitative assessment

In calbindin immunolabelled sections, quantitative analysis of the distribution of positive cell labelling was carried out as previously described [12]. In brief, images were captured at ×10 magnification on calbindin stained sections with a Zeiss Axio microscope (Zeiss, Cambridge, UK). Up to

Table 1. Grading system for assessment of neuronal loss and evaluation of mossy fibre sprouting (MFS) on dynorphin staining and alterations to inhibitory neuronal markers in the dentate gyrus

Grade	*0*	*1*	*2*	*3*
CA1	No neuronal loss	Neuronal loss present but incomplete (~50–75%)	Majority of neurones lost (>75%)	
CA4	No neuronal loss	Neuronal loss present but incomplete (~50–75%)	Majority of neurones lost (>75%)	
GCD	Normal granule cell layer	Mild dispersion	Severe dispersion	
Dynorphin	Normal pattern: labelling of the mossy fibre pathway in CA4 and CA3	MFS in IML	MFS in IML and OML	
Neuropeptide Y	Normal pattern: radial axonal sprouts inconspicuous & horizontal axonal network in OML > IML	Few radial axonal sprouts in IML but gradient between IML and OML still visible.	Radial axonal sprouts prominent and gradient between IML and OML not visible	As in grade 2 but radial axonal sprouts through IML OML and SGZ
Calretinin	Normal pattern: dense band of axons in immediate SGZ and IML	Loss of SGZ labelling	Diminution of dense band of axons in SGZ and IML and axonal sprouts	As in grade 2 but extensive axonal sprouts in IML and OML
Calbindin	Normal pattern: strong expression in granule cells, apical dendrites and mossy fibres in CA4 and CA3	Patchy loss of expression in granule cells	Majority of granule cells negative	Loss of expression predominates in basal cell layer

These grading schemes are based on previously used and validated scoring schemes [12–14,23]. Granule cell depletion was not recorded in this system. GCD, granule cell dispersion; MFS, mossy fibre sprouting; IML, internal molecular layer; OML, outer molecular layer; SGZ, subgranular zone.

8 fields along the dentate gyrus were selected per case, avoiding angles and curvatures. Using Image-Pro software (version 6.3, Media Cybernetics, UK), the perpendicular distances of cells (μm) in the dentate gyrus was measured from a line drawn along the basal granule cell layer in each image. This was repeated for positively and negatively stained granule cells in each region. The mean distance for each group of cells and the differences between these means was recorded.

Statistical analysis of data between groups was carried out with SPSS (IBM, version 20) using the Mann-Whitney test and Pearson's correlation.

Results

Patterns of HS and GCD

Neuronal loss in the HS_D group was predominantly centred on CA1, rather than CA4 subfield, compared with HS_E cases (Table S1, Table 2; Figure 1**A**); a significant difference in the severity of neuronal loss in CA4, but not CA1, was shown for all HS_D (AD + FTLD) compared to HS_E ($P < 0.0001$). Additionally, in four HS_D cases the neuronal loss in CA1 continued into the subiculum, whereas in HS_E cases, there was an abrupt transition between neuronal loss in CA1 and the spared subiculum (Figure 1**B**). In one HS_D case, the neuronal loss was restricted to a segment of CA1. GCD was less pronounced in the HS_D group (Table 2) with over 80% showing no dispersion, compared to 44% with no dispersion in the HS_E group (Figure 1**A**,**B**). GFAP in HS_E (Figure 1**D**) showed a typical pattern of dense fibrous gliosis relatively restricted to CA1 and CA4, sparing CA2 and subiculum, with radial glial fibres in the dentate gyrus. In HS_D cases patterns of gliosis were more variable between subfields, as previously noted [24], but in the majority of cases a cellular astrocytosis was equally or more pronounced in the subiculum than CA1, and radial gliosis was less consistently present in the dentate gyrus. In GFAP-δ immunostained sections in both HS_D and HS_E prominent reactive glia were noted in the subgranular zone and CA4 to a greater extent than CA1, as previously described in HS_E [25] (Figure 1**C**,**D**); delta-GFAP was therefore less discriminatory than GFAP in the evaluation of HS types.

*Dynorphin (Figure 1**G**,**H**; Figure 2**A–C**)* In HS_E, MFS was confirmed in five cases, with grade 2 sprouting observed in four; there was no MFS in any of the controls. Dynorphin immunolabelling confirmed a normal mossy fibre

Table 2. Results of hippocampal pathology, shown as percentage of cases with each grade in the patient groups (see text and Table 1 for details of grading scheme)

	CA1			*CA4*			*Dynorphin*			*Calbindin*				*Calretinin*				*Neuropeptide Y*				*GCD*		
Grade	*0*	*1*	*2*	*0*	*1*	*2*	*0*	*1*	*2*	*0*	*1*	*2*	*3*	*0*	*1*	*2*	*3*	*0*	*1*	*2*	*3*	*0*	*1*	*2*
HS_E ($n = 9$)	0%	33%	67%	11%	44%	44%	37.5%	12.5%	50%	0%	11%	33%	56%	29%	14%	0%	57%	12.5%	25%	0%	62.5%	44%	11%	45%
HS_D AD ($n = 10$)	6%	50%	44%	83%	17%	0%	90%	10%	0%	30%	50%	0%	20%	60%	20%	20%	0%	20%	60%	20%	0%	83%	17%	0%
HS_D FTLD ($n = 8$)							71%	29%	0%	62.5%	25%	12.5%	0%	75%	12.5%	12.5%	0%	57%	43%	0%	0%			
Control cases ($n = 11$)	91%	9%	0%	91%	9%	0%	100%	0%	0%	67%	22%	11%	0%	100%	0%	0%	0%	100%	0%	0%	0%	100%	0%	0%
Significance*	$P = 0.05$			$P < 0.0001$			$P = 0.01$			$P = 0.005$				$P = 0.002$				$P = 0.01$				$P = 0.05$		

n = the number of cases in each group. With some antibodies, occasional cases were not included in the analysis due to repeated technical problems. *Significance is shown as between grades in all HS_E and HS_D (AD + FTLD) groups using the Mann–Whitney test. HS_E, hippocampal sclerosis with epilepsy; HS_D, hippocampal sclerosis with dementia; AD, Alzheimer's disease; FTLD, fronto-temporal lobe dementia; GCD, granule cell dispersion.

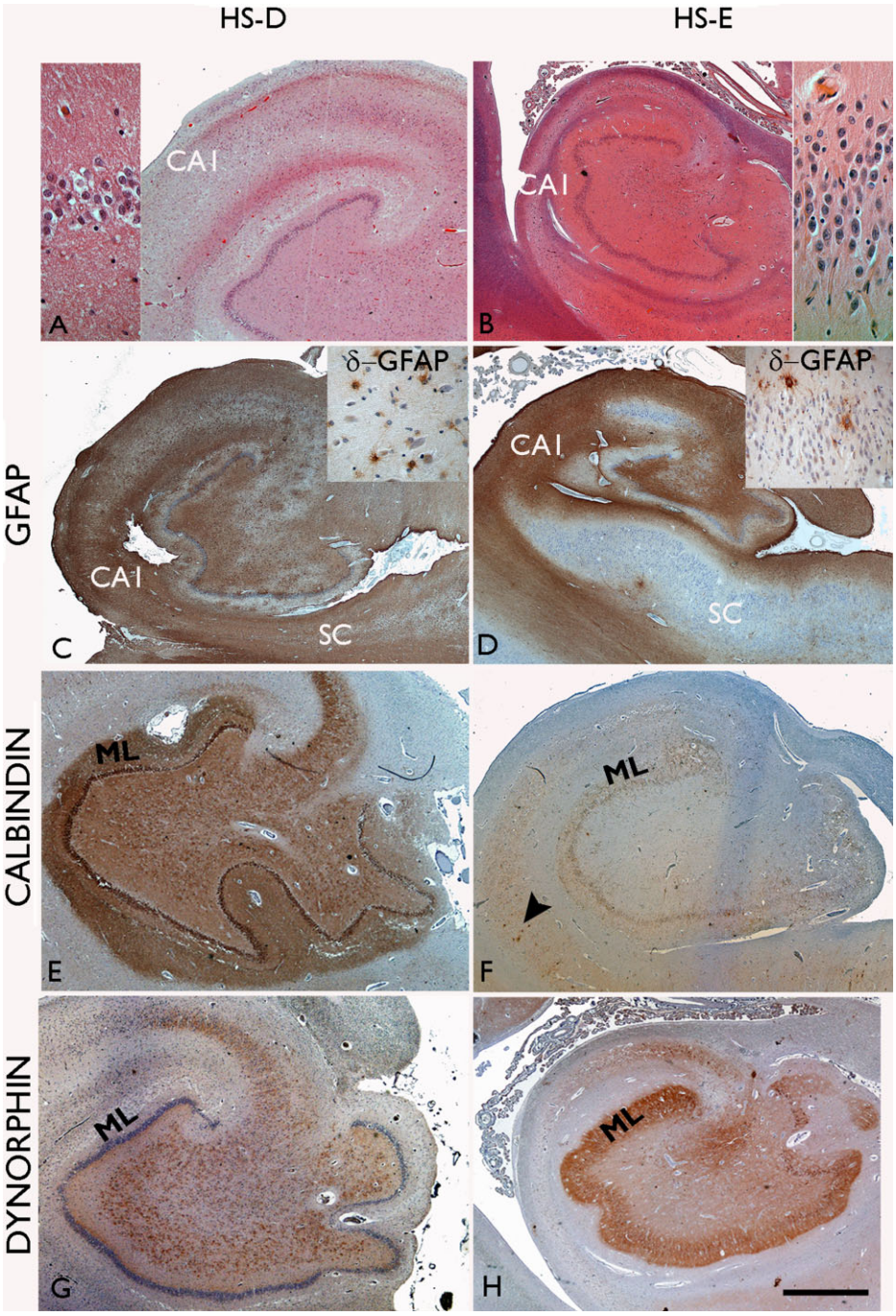

Figure 1. Comparison of hippocampal pathology in hippocampal sclerosis with dementia (HS_D; **A**,**C**,**E**,**G**) and with epilepsy (HS_E; **B**,**D**,**F**,**H**). In both HS_D and HS_E neuronal loss in CA1 is the predominant finding (**A**,**B**); dispersion of the granule cells is more commonly a feature accompanying HS_E (**B**, insert) than HS_D (**A**, insert). Astrocytic gliosis with GFAP immunostaining is more variable and cellular, but can be extensive in HS_D and can be equally severe in the subiculum (SC) as in CA1 (**C**); in HS_E there is abrupt, subfield-specific fibrous gliosis demarcating CA1 and CA4 with sparing of the subiculum (SC) and CA2 region. With delta-GFAP immunostaining in HS_D and HS_E (insets in **C**,**D** respectively), scattered multi-polar glial cells are prominent in CA4 and near the basal granule cell layer. (**E**) Normal calbindin staining is shown in the hippocampus with labelling of granule cell layer, apical dendrites in the molecular layer (ML) and axonal projection in the mossy fibre pathway to CA4 and CA3. (**F**) In HS_E loss of calbindin expression in the granule cells and their processes is a frequent finding but with residual interneurones normally labelling (arrow). (**G**) A normal dynorphin immunostaining pattern in HS_D highlighting the mossy fibre pathway and (**H**) mossy fibre sprouting in the molecular layer (ML) in HS_E. Bar in all approximately equivalent to 2500 μm.

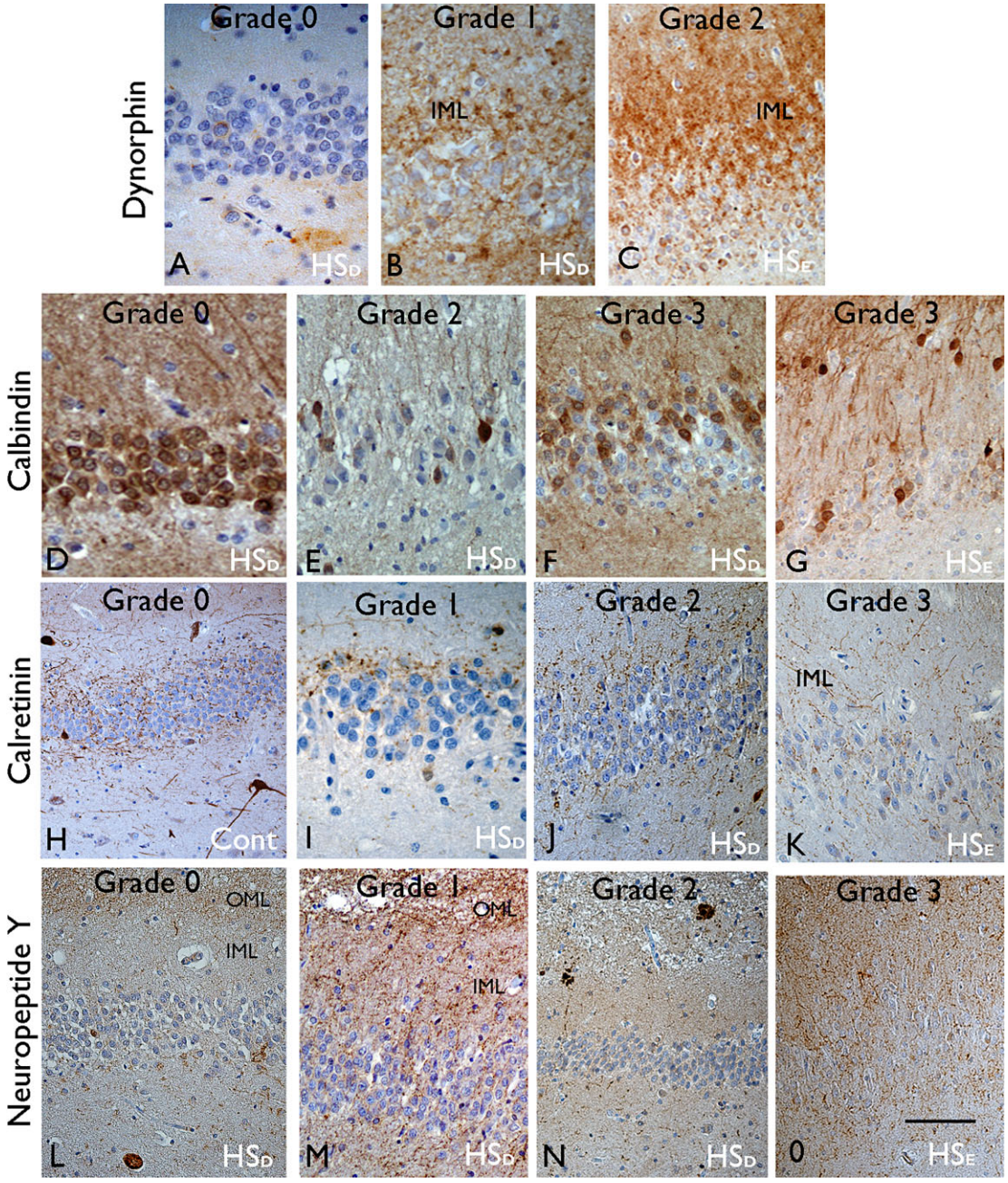

Figure 2. Dentate gyrus alterations in hippocampal sclerosis in epilepsy (HS_E) and dementia (HS_D) and control (cont). Dynorphin: (**A**) In the majority of HS_D cases a normal mossy fibre pathway (grade 0) was visible with labelling of axons in CA4 and no immunopositivity visible in the molecular layer. (**B**) Occasional focal sprouting of dynorphin-positive fibres was noted in the inner molecular layer (IML) in three HS_D (grade 1). (**C**) Severe and extensive mossy fibre sprouting (grade 2) in the molecular layer (IML) was seen only in HS_E cases. Calbindin: (**D**) Normal expression in granule cells, dendrites and mossy fibre axons was noted in controls and HS_D cases (grade 0) with, (**E**) loss of expression in some cases (grade 2). (**F**) Loss of expression restricted to basal granule cells (grade 3) was noted in three HS_D cases without dispersion and (**G**) was the commonest pattern in HS_E cases with granule cell dispersion. Calretinin: (**H**) a normal pattern of calretinin labelling of the axonal plexus on either side of the granule cell layer is shown in controls (grade 0). (**I**) Loss of the plexus in the subgranular zone (grade I) and (**J**) sprouting of fibres in the IML (grade 2) was seen in some HS_D cases. (**K**) In HS_E, marked sprouting of fibres in the IML was a prominent finding (grade 3). Neuropeptide Y: (**L**) Normal pattern (grade 0) with an axonal plexus in the outer molecular layer (OML) was seen in controls. Progressively more prominent sprouting of fibres was noted in the inner molecular layer (IML) in HS_D cases (grade 1 to 2; **I**,**J**). (**O**) Extensive NPY fibre sprouting through the molecular layer (grade 3) was only observed in HS_E. See also Table 1 for details of descriptions of grading. Bar is equivalent to 300 μm.

pathway in the majority of HS_D cases, with only three cases showing MFS, one in the AD group (grade 1) and two in the FTLD group (grade 1) (Table S1, Table 2); no grade 2 MFS was noted in the HS_D group. Of note, in contrast to the loss of dynorphin labelling of axons and terminals in the normal mossy fibre projection to CA4 and CA3 in HS_E cases with MFS, in HS_D these pathways appeared better preserved. In addition, in one AD case, plaque-like aggregates of dynorphin were noted in the CA4 region (Figure 3**A**), likely corresponding to neuritic plaques.

Calbindin (Figure 1E,F; Figure 2D–G) Reduced calbindin expression was noted in the granule cells in all HS_E cases, the predominant pattern being grade 3, with loss of expression restricted to the more basal cells, as reported previously [12]. In addition, prominent sprouting of calbindin-positive fibres through the dentate gyrus was noted in four cases (Figure 3**B**) as previously described in epilepsy [11]. Loss of calbindin was statistically less frequent in HS_D (Figure 2**D–E**), observed in 10 of the 18 cases (seven from the AD group); Only two cases had a grade 3 pattern with the loss of calbindin in the more basal cells compared to the distal cells (Figure 2**F**), but in contrast to HS_E this was not accompanied by GCD (Table 2). Measurements confirmed greater mean differences in the position of positive *vs.* negatively labelled granule cells from the basal layer in HS_E than HS_D or control groups (mean values 30.2, 10.1 and −3.9 μm respectively; $P < 0.05$). Sprouting of calbindin-positive axon fibres was not observed in any HS_D cases. The loss of calbindin in granule cells was also present in three controls. In all cases with reduced expression of calbindin in the hippocampal granule cells, normal interneuronal staining was preserved in the adjacent cortex.

Calretinin (Figure 2H–K) The predominant pattern in HS_E was grade 3 (4 cases), with prominent sprouting of fibres and loss of the normal organization (Table 2, Figure 2**K**). All controls showed a normal calretinin pattern (Figure 2**H**). Abnormal calretinin pattern was seen in six of the 18 HS_D cases (grade 2 (three cases) and grade 1 (three cases); 4 in the AD group) (Figure 2**I–J**) but no grade 3 patterns were observed. In a further case, loss of calretinin labelling in the dentate gyrus was noted. Calretinin interneurons appeared generally preserved and normal in appearance in the adjacent temporal cortex in AD and FTLD cases.

Neuropeptide Y (Figure 2L–O) The predominant pattern in the HS_E was grade 3, with prominent sprouting of fibres through the dentate gyrus (Figure 1**O**); a normal NPY pattern was seen in only one case. Controls all showed a normal NPY pattern. In HS_D cases, NPY patterns were abnormal in 11 cases [grade 2 (two cases) and grade 1 (nine cases)] (Figure 1**L–N**); no grade 3 pattern was observed. Occasional NPY processes were seen within senile plaques (Figure 2**N**).

Statistical analysis confirmed significantly higher grades of reorganization of calbindin, calretinin, NPY and dynorphin labelling in the dentate gyrus in HS_E compared to all HS_D cases (Table S1 and Table 2). There were strong correlations between calretinin, NPY and dynorphin grades (but not calbindin) in the HS_E group (all $P < 0.001$), but this was less evident in the HS_D group (all $P > 0.01$). In eight cases in the HS_D group, abnormal patterns were observed in the dentate gyrus with two or more of the four markers and in two cases (one AD, one FTLD) with all four. In one HS_D patient with a history of seizures, grade 1 patterns were seen with calbindin and NPY but dynorphin and calretinin patterns were normal. There were no statistical differences in any of the pathological measures between HS_E patients with or without cognitive decline, but the numbers in each group were small; similarly no differences were noted between the HS_D AD and FTLD groups.

An additional finding on NPY sections was the prominent labelling of structures resembling Hirano bodies in 12 HS_D cases (8 AD, 4 FTLD) (Figure 3**D–E**). They were regionally restricted to CA1 sector, not seen in other subfields or the neocortex, and their presence was confirmed on corresponding H&E sections (Figure 3**C**). NPY-positive Hirano bodies were observed adjacent to remaining pyramidal cell somata or 'free' in the neuropil (Figure 3**D–E**). NPY-positive processes were visible as a 'tail'-like extension from some Hirano bodies (Figure 3**E**) and a central unlabelled core was noted for some bodies imparting ring-like structures. In seven cases, Hirano body-like structures were visible on calretinin-labelled sections but not with calbindin or dynorphin labelling (Figure 3**G**). Double-labelling immunofluorescence of NPY with dendritic marker, anti-MAP2, confirmed focal co-localization in some Hirano bodies (Figure 3**I**), whereas others appeared lying adjacent to, but distinct from, phosphorylated tau (AT8)-positive pyramidal cells (Figure 2**H**). We did not see Hirano bodies co-localizing with neurofilament-positive axons (not shown). NPY (or calretinin)-labelled Hirano

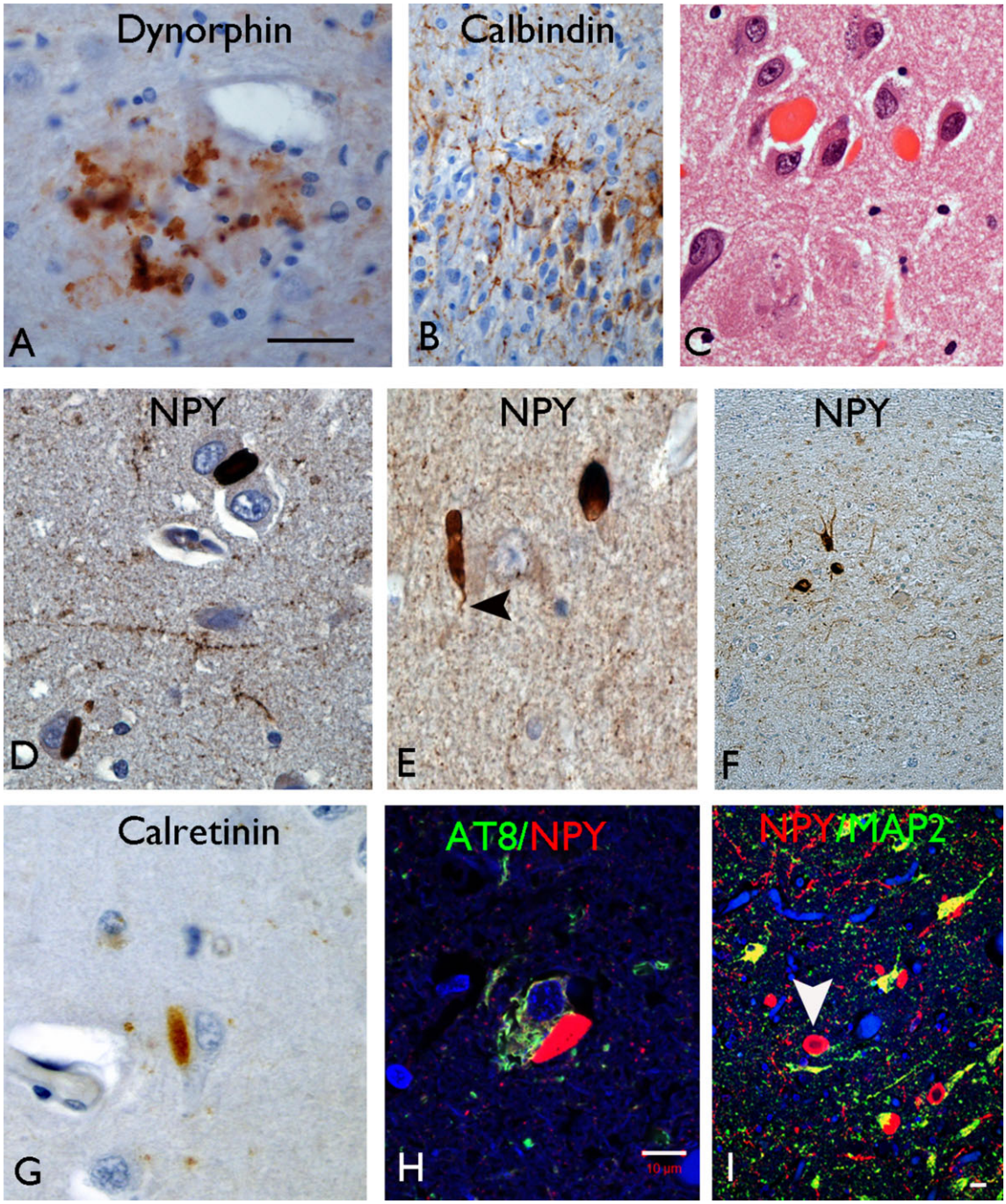

Figure 3. (**A**) Dynorphin occasionally labelled neuritic plaques in CA4 in Alzheimer's disease cases. (**B**) Sprouting of calbindin-positive fibres was noted in the dentate gyrus in HS_E cases but not in HS_D. (**C**) Hirano bodies were noted in CA1 in the control and HS_D groups but not in HS_E on H&E preparations. (**D**) NPY showed intense labelling of numerous Hirano body-like structures in CA1 in HS_D in addition to labelling axons and residual interneurons in this region. They were seen in proximity to negatively labelled pyramidal neurones (**D**) or free in the neuropil (**E**) with occasional body showing a tail like process (arrowhead in **E**). (**F**) In HS_E cases, only interneurons and extensive fibre networks were labelled in CA1 with NPY. (**G**) Weaker labelling of Hirano bodies was noted with calretinin. (**H**) Con-focal microscopy showed no co-localization of NPY-positive Hirano-like bodies with AT8 positive pyramidal cells in CA1; double-labelling with dendritic marker MAP2 (**I**) showed approximation of NPY Hirano bodies to neuronal process and dendrites. In addition, a peripheral rim of NPY positivity was appreciated in some Hirano bodies with a hollow central core (arrowhead). Bars in **A**,**C**,**D**,**E**,**G** = 75 µm, **B**,**F** = 140 µm, **H** = 20 µm, **I** = 20 µm.

bodies were not seen with any of the epilepsy cases (even up to age 87 years), where only normal NPY interneurons were observed (Figure 3**F**). NPY-positive Hirano bodies were noted in CA1 in three controls (57–68 years).

Discussion

Hippocampal sclerosis is a generic term used for the description of neuronal loss and gliosis, preferentially involving hippocampal subfields. Although historically associated with epilepsy, there has been increasing recognition in recent years of a similar pathological change arising as a 'pure' lesion in elderly, or in association with a neurodegenerative condition. These different clinical groups of HS have not been directly compared histologically. Identification of different cellular alterations would be helpful in their diagnostic evaluation, would allow a deeper understanding of different mechanisms of cell degeneration that may be operating, and would enable the identification of pathological alterations that correlate with specific clinical symptoms, for example cognitive dysfunction *vs.* hippocampal epileptogenicity.

HS_E and HS_D may both be bilateral or asymmetrical between hemispheres [23,26], with no clear predilection for left or right and may vary in the extent of its longitudinal involvement along the hippocampal axis (Table 3). In this present study we focused on one level of the hippocampal body from each case, representative of the sclerosis, for detailed analysis. We observed differences between HS_D and HS_E in the distribution of cell loss

Table 3. Summary of the clinical, pathological and aetiological features that enable the distinction of HS_E from HS_D

Feature	*HS in epilepsy (HS_E)*	*HS in dementia and ageing (HS_D)*
Clinical context		
Typical presentation	Childhood to young adulthood Seizure syndromes, particularly mTLE	Adult to the 'oldest-old' Dementia, cognitive decline.
Prevalence	Surgical epilepsy series ~35% PM epilepsy series ~30–40%	In elderly between ~3–24% 'Pure' HS in 23% of dementia cases
Distribution		
Bilaterality	Bilateral in ~48–56% in epilepsy PM series (all syndromes including TLE)	Bilateral in ~45–60%
Longitudinal extent	Localized or extensive along rostro-caudal length [14]	Localized or extensive along rostro-caudal length [26]
Pattern of HS		
Distribution of neuronal loss and gliosis	CA1: Typically severe cell loss Subiculum: Spared CA4/3: Neuronal loss Granule cell dispersion in ~50%	CA1: Extensive to patchy loss Subiculum: Often cell loss CA4: Spared Granule cell dispersion less evident
Circuitry reorganization		
Mossy fibre system	Mossy fibre sprouting typically present and extensive	Mossy fibre sprouting usually absent If present mild and focal
Calbindin expression	Reduced expression in granule cells, particularly basal cells	Reduced expression in granule cells may occur
NPY expression	Resistance of CA1 interneurones Prominent sprouting in DG	Loss of CA1 interneurones Mild sprouting in DG in some
Calretinin	Reorganization of DG networks	Mild reorganization of DG networks may be present
Patho-mechanisms		
Causes of neuronal loss	Seizure mediated/excitotoxic neuronal injury	Heterogenous causes: 'Ageing' Vascular brain injury AD, FTLD Synucleinopathies with HS
Contribution of TDP-43, ApoE	TDP-43 not identified in surgical unilateral cases [17,59] or bilateral HS_E at PM [5] *ApoE* ε4 associated with earlier onset [60] in some but not all studies [61]	TDP-43 inclusions in up to 93% of pure HS_D [17,47] [26] HS_D not associated with *ApoE* ε4 [17,47]

mTLE, mesial temporal lobe epilepsy; DG, dentate gyrus; HS, hippocampal sclerosis; PM, *post mortem*; AD, Alzheimer's disease; FTLD, frontotemporal lobe dementia.

between subfields at this coronal level. The neuronal loss in HS_D predominantly involved CA1 sector, typically extending into the subiculum in several cases, but sparing CA4. This distribution of neuronal loss has been previously reported in studies of HS_D [17,26]. This contrasts to the classical pattern of atrophy in HS_E, where CA1 damage is accompanied by CA4 neuronal loss with an abrupt transition between the neuronal loss and gliosis in CA1 and the adjacent well-preserved subiculum [1]. We also showed that GCD, a common alteration in HS_E [27,28], was rare and mild in HS_D. GCD has been associated with both an early age of onset of seizures and with the severity of CA4 neuronal loss [27,29]. An atypical pattern of HS_E shows predominant involvement of CA1 only, and has been associated with a later age of onset of seizures [30,31]. These observations could indicate an age-dependent vulnerability of the dentate gyrus and CA4, which is spared in older onset HS_E and HS_D cases.

Studies of HS in epilepsy series have focussed on cellular alterations that could render this region hyper-excitable. MFS was first observed in experimental seizure models as an early event [8] and has been suggested to be critical to the development of recurrent seizure activity associated with HS_E, through enhanced excitability and/or synchronization of granule cells. We have previously shown, in a PM series of HS_E cases, that MFS can persist into the ninth decade, even with the remission of seizures [23]. Therefore, there is an alternative argument that MFS is an epiphenomenon or response to seizures, rather than a primary epileptogenic process. In one HS_D patient in the present series in whom occasional clinical seizures were documented, MFS was not present and in other HS_D cases, MFS was rare and mild. In elderly patients and those with cognitive decline, partial seizures may be unrecognized [32,33] because EEG may not be performed as a routine test, therefore we cannot entirely exclude 'sub-clinical' seizure activity as the mechanism for the focal MFS seen in HS_D. Notwithstanding, the findings favour the view that severe MFS is linked with hippocampal excitability and is therefore a relatively reliable histological marker for HS_E.

Alterations to dentate gyrus interneurones have been extensively studied in HS_E, in surgical and PM tissues. Cell loss, cyto-morphological alterations and axonal sprouting represent the more common findings (for review see [34]) and these stereotypical alterations parallel the principal neuronal loss in established cases [14]. Interneuronal alterations are not exclusive to HS_E associated with mTLE, and can be seen with other epilepsy syndromes [14,23]. It is the axonal sprouting of interneurons that is considered a more functionally significant process in relation to network changes, correlating with synaptic re-organization [9,11]. These alterations are easily recognized and reliably graded in tissue sections, as in the present study, and sprouting of these inhibitory networks in the dentate gyrus tend to occur in synchrony with the sprouting of excitatory networks (the mossy fibres) [23]. We identified significantly more cases with interneuronal sprouting using calretinin and NPY labelling in HS_E than HS_D cases with more extensive sprouting (corresponding to the higher grades) as well as sprouting of calbindin-positive fibres, which was exclusive to HS_E cases.

In previous studies of the hippocampus in AD, a reduction of NPY axons in the dentate gyrus was demonstrated, with clusters or beaded clumps of axons, some associated with neuritic plaques [35]. We also confirmed occasional association of NPY fibres in addition to dynorphin fibres, associated with neuritic plaques in AD. In an APP-mutant model of AD, ectopic expression of NPY was shown in granule cells as well as sprouting of NPY fibres in the molecular layer from hilar NPY neurones [36]. The authors proposed that this represented amyloid β-mediated neuronal excitatory activity and subsequent re-modelling of inhibitory circuits that resemble alterations in experimental epilepsy models [36]. Our study supports the notion that subtle inhibitory neuronal network alterations may occur in HS_D, similar to HS_E. As for our observations with MFS in HS_D, we cannot exclude subclinical epileptic activity or un-recognized seizures and local hippocampal excitability as a cause for these alterations. Furthermore, in eight of the HS_D cases with MFS and interneuronal alterations, parallel changes were seen with more than one marker, supporting systematic network re-organization occurring in the dentate gyrus in some cases. A further consideration is that the cellular pathology occurring in HS with neurodegeneration could inhibit these synaptic reorganizational changes that are more profuse in HS with epilepsy.

Loss of calbindin expression in the dentate granule cells has been shown in experimental AD models (human APP transgenic mutant) as well as in PM series [37–39] and correlated with both cognitive deficits and the abundance of amyloid β protein [40]. Loss of calbindin in AD was the most frequent abnormality, observed in 70% of AD HS_D compared to 37% in the FTLD group in this study. It is also known that an age-related decline of calbindin in granule cells occurs, which has been associated with impaired

hippocampal function [41], and was noted in three controls in the current study. We recently reported a pattern of calbindin loss from the basal granule cells in HS_E associated with early onset of seizures, which was the most prominent pattern also in the present HS_E cases. This pattern was noted in only two of the HS_D cases. It has been proposed that loss of calbindin causes changes to the intrinsic excitability of granule cells in addition to its roles in memory impairment [42]. A reduction of CA4 calretinin positive neurones has also been shown in experimental [43] and AD cases [44], although less is known about hippocampal interneuronal alterations in FTLD [45]. Calretinin axonal networks have not been previously studied in HS_D; they were mildly altered in a minority of cases in the present series.

HS_D may be encountered as a 'pure' or isolated pathology in the elderly, associated with dementia or an amnestic syndrome and in the absence of typical neuronal inclusions associated with AD or FTLD or vascular disease. This may represent a relatively unrecognized cause of dementia, in the oldest age groups [46] and is associated with TDP-43 immunoreactive inclusions in the granule cells [17,26,47]. The present study was limited by not having 'pure' HS_D cases available for comparison to HS_E. Nevertheless from a practical viewpoint, when HS is encountered at PM examination in the elderly, the pattern of neuronal loss in addition to assessment of any neurodegenerative features (including TDP-43), interneuronal markers and mossy fibre alterations may help to identify the cause of the sclerosis (as summarized in Table 3).

A serendipitous finding in the study was the labelling of Hirano bodies in AD and controls for NPY and, to a lesser extent, calretinin. The origin and physiological function of Hirano bodies in ageing and AD has remained elusive since their first recognition 40 year ago. They are filamentous, paracrystalline inclusions, comprising many proteins including actin, co-filin and alpha-actinin [48,49]. The focal overlap of expression of the NPY-positive Hirano body with MAP2 supports the view that some are within dendrites, as previously reported [48,50], whereas others may be axonal. It is estimated that CA1 pyramidal cells are supported by 16 types of GABA-ergic neurones [51], including NPY interneurons, many forming a connected 'pair' with a single CA1 pyramidal cell [52]. NPY-positive interneurons in CA1 are *bi-stratified* cells with axon terminals on the dendritic domains of CA1 pyramidal cells, mediating inhibition via $GABA_A$ receptors [51,53]. The NPY cell dendrites extend into the stratum oriens and radiatum and, in turn, receive excitatory input from pyramidal cell collaterals.

Previous studies of CA1 NPY interneurones in AD described the most dramatic changes occurring in this subfield with surviving cells bearing shortened dendrites ('dendritic stumps') and damaged thick axons, although labelling of Hirano bodies was not described [35,54]. In the PS1/APP transgenic model of AD, loss of NPY-somatostatin co-labelled neurones in CA1 was an early finding, demonstrating a specific vulnerability of these cells in AD, which preceded the pyramidal cell loss [55]. In HS_E by contrast, relative resistance of NPY-positive interneurons in CA1 has been shown [56] in epilepsy models and in human MTLE/HS cases, despite the extensive loss of CA1 pyramidal cells and hilar NPY cells [31]. These observations highlight a different time-course for loss of CA1 NPY interneurons in HS_D due to AD *vs.* HS_E. Recent studies have shown PSD-95, a structural protein of excitatory synapses, to label a proportion of Hirano bodies [50]; a further study showed co-localization of Hirano bodies with GluR1 and R2 AMPA receptors in the vicinity of pyramidal cells [57]. It has been postulated Hirano bodies represent aberrant formation of post-synaptic structures in response to distal synaptic destruction [50]. In experimental systems, Hirano bodies have been shown to be both protective against neurodegeneration mediated by tau or APP [58] as well as to inhibit normal cellular function [49]. One explanation is that Hirano bodies arise in residual NPY neurones in AD as a compensatory, but cellular degenerative response, to the ongoing imbalances between reciprocal inhibitory and excitatory networks as the disease progresses. The potential functional significance of Hirano bodies is therefore of interest and requires further study.

In summary, reorganization of excitatory and inhibitory networks in the dentate gyrus is more typical of HS_E. Subtle alterations may occur in HS_D, which could be a result of increased hippocampal excitability, including unrecognized seizure activity. An unexpected finding was the identification of NPY-positive Hirano bodies in HS_D but not HS_E, which may be a consequence of the relative vulnerabilities of interneurons in these conditions.

Acknowledgements

We are grateful to Queen Square Brain Bank for the donation of tissues, in particular to Linda Parsons and Hilary Ailing. This work was undertaken at UCLH/UCL, which

received a proportion of funding from the Department of Health's NIHR Biomedical Research Centres funding scheme. JL is supported by a grant from the MRC (G0600934). The authors have no conflicts of interest to declare. RB carried out the laboratory work, quantitative analysis and contributed to the manuscript preparation; JL carried out all double labelling and confocal analysis and developed the immunohistochemistry protocols; SMS contributed to the clinical data collection; MT contributed with the study design, data analysis and the manuscript preparation. We confirm that we have read the Journal's position on issues involved in ethical publication and affirm that this report is consistent with those guidelines.

References

1 Blumcke I, Coras R, Miyata H, Ozkara C. Defining clinico-neuropathological subtypes of mesial temporal lobe epilepsy with hippocampal sclerosis. *Brain Pathol* 2012; **22**: 402–11
2 Labate A, Gambardella A, Andermann E, Aguglia U, Cendes F, Berkovic SF, Andermann F. Benign mesial temporal lobe epilepsy. Nature reviews. *Neurology* 2011; **7**: 237–40
3 Semah F, Picot MC, Adam C, Broglin D, Arzimanoglou A, Bazin B, Cavalcanti D, Baulac M. Is the underlying cause of epilepsy a major prognostic factor for recurrence? *Neurology* 1998; **51**: 1256–62
4 Bonilha L, Martz GU, Glazier SS, Edwards JC. Subtypes of medial temporal lobe epilepsy: influence on temporal lobectomy outcomes? *Epilepsia* 2012; **53**: 1–6
5 Thom M, Liu JY, Thompson P, Phadke R, Narkiewicz M, Martinian L, Marsdon D, Koepp M, Caboclo L, Catarino CB, Sisodiya SM. Neurofibrillary tangle pathology and Braak staging in chronic epilepsy in relation to traumatic brain injury and hippocampal sclerosis: a post-mortem study. *Brain* 2011; **134**: 2969–81
6 Thom M. Hippocampal sclerosis: progress since Sommer. *Brain Pathol* 2009; **19**: 565–72
7 Houser CR. Granule cell dispersion in the dentate gyrus of humans with temporal lobe epilepsy. *Brain Res* 1990; **535**: 195–204
8 Sutula T, Cascino G, Cavazos J, Parada I, Ramirez L. Mossy fiber synaptic reorganization in the epileptic human temporal lobe. *Ann Neurol* 1989; **26**: 321–30
9 Magloczky Z. Sprouting in human temporal lobe epilepsy: excitatory pathways and axons of interneurons. *Epilepsy Res* 2010; **89**: 52–9
10 Magloczky Z, Halasz P, Vajda J, Czirjak S, Freund TF. Loss of calbindin-D28K immunoreactivity from dentate granule cells in human temporal lobe epilepsy. *Neuroscience* 1997; **76**: 377–85
11 Magloczky Z, Wittner L, Borhegyi Z, Halasz P, Vajda J, Czirjak S, Freund TF. Changes in the distribution and connectivity of interneurons in the epileptic human dentate gyrus. *Neuroscience* 2000; **96**: 7–25
12 Martinian L, Catarino CB, Thompson P, Sisodiya SM, Thom M. Calbindin D28K expression in relation to granule cell dispersion, mossy fibre sprouting and memory impairment in hippocampal sclerosis: a surgical and post mortem series. *Epilepsy Res* 2012; **98**: 14–24
13 Mathern GW, Babb TL, Pretorius JK, Leite JP. Reactive synaptogenesis and neuron densities for neuropeptide Y, somatostatin, and glutamate decarboxylase immunoreactivity in the epileptogenic human fascia dentata. *J Neurosci* 1995; **15**: 3990–4004
14 Thom M, Liagkouras I, Martinian L, Liu J, Catarino CB, Sisodiya SM. Variability of sclerosis along the longitudinal hippocampal axis in epilepsy: a post mortem study. *Epilepsy Res* 2012; **102**: 45–59
15 Probst A, Taylor KI, Tolnay M. Hippocampal sclerosis dementia: a reappraisal. *Acta Neuropathol* 2007; **114**: 335–45
16 Zarow C, Sitzer TE, Chui HC. Understanding hippocampal sclerosis in the elderly: epidemiology, characterization, and diagnostic issues. *Curr Neurol Neurosci Rep* 2008; **8**: 363–70
17 Nelson PT, Schmitt FA, Lin Y, Abner EL, Jicha GA, Patel E, Thomason PC, Neltner JH, Smith CD, Santacruz KS, Sonnen JA, Poon LW, Gearing M, Green RC, Woodard JL, Van Eldik LJ, Kryscio RJ. Hippocampal sclerosis in advanced age: clinical and pathological features. *Brain* 2011; **134**: 1506–18
18 Dickson DW, Davies P, Bevona C, Van Hoeven KH, Factor SM, Grober E, Aronson MK, Crystal HA. Hippocampal sclerosis: a common pathological feature of dementia in very old (> or = 80 years of age) humans. *Acta Neuropathol* 1994; **88**: 212–21
19 Montine TJ, Phelps CH, Beach TG, Bigio EH, Cairns NJ, Dickson DW, Duyckaerts C, Frosch MP, Masliah E, Mirra SS, Nelson PT, Schneider JA, Thal DR, Trojanowski JQ, Vinters HV, Hyman BT. National Institute on Aging-Alzheimer's Association guidelines for the neuropathologic assessment of Alzheimer's disease: a practical approach. *Acta Neuropathol* 2012; **123**: 1–11
20 Mackenzie IR, Neumann M, Baborie A, Sampathu DM, Du Plessis D, Jaros E, Perry RH, Trojanowski JQ, Mann DM, Lee VM. A harmonized classification system for FTLD-TDP pathology. *Acta Neuropathol* 2011; **122**: 111–3
21 Liu JY, Martinian L, Thom M, Sisodiya SM. Immunolabeling recovery in archival, post-mortem, human brain tissue using modified antigen retrieval and the catalyzed signal amplification system. *J Neurosci Methods* 2010; **190**: 49–56
22 Liu JY, Thom M, Catarino CB, Martinian L, Figarella-Branger D, Bartolomei F, Koepp M, Sisodiya SM. Neuropathology of the blood-brain barrier and

pharmaco-resistance in human epilepsy. *Brain* 2012; **135**: 3115–33
23 Thom M, Martinian L, Catarino C, Yogarajah M, Koepp MJ, Caboclo L, Sisodiya SM. Bilateral reorganization of the dentate gyrus in hippocampal sclerosis: a postmortem study. *Neurology* 2009; **73**: 1033–40
24 Miyata H, Hori T, Vinters HV. Surgical pathology of epilepsy-associated non-neoplastic cerebral lesions: a brief introduction with special reference to hippocampal sclerosis and focal cortical dysplasia. *Neuropathology* 2013; **33**: 442–58
25 Martinian L, Boer K, Middeldorp J, Hol EM, Sisodiya SM, Squier W, Aronica E, Thom M. Expression patterns of glial fibrillary acidic protein (GFAP)-delta in epilepsy-associated lesional pathologies. *Neuropathol Appl Neurobiol* 2009; **35**: 394–405
26 Zarow C, Weiner MW, Ellis WG, Chui HC. Prevalence, laterality, and comorbidity of hippocampal sclerosis in an autopsy sample. *Brain Behav* 2012; **2**: 435–42
27 Blumcke I, Kistner I, Clusmann H, Schramm J, Becker AJ, Elger CE, Bien CG, Merschhemke M, Meencke HJ, Lehmann T, Buchfelder M, Weigel D, Buslei R, Stefan H, Pauli E, Hildebrandt M. Towards a clinico-pathological classification of granule cell dispersion in human mesial temporal lobe epilepsies. *Acta Neuropathol* 2009; **117**: 535–44
28 Wieser HG. ILAE Commission Report. Mesial temporal lobe epilepsy with hippocampal sclerosis. *Epilepsia* 2004; **45**: 695–714
29 Thom M, Liagkouras I, Elliot KJ, Martinian L, Harkness W, McEvoy A, Caboclo LO, Sisodiya SM. Reliability of patterns of hippocampal sclerosis as predictors of postsurgical outcome. *Epilepsia* 2010; **51**: 1801–8
30 Blumcke I, Pauli E, Clusmann H, Schramm J, Becker A, Elger C, Merschhemke M, Meencke HJ, Lehmann T, von Deimling A, Scheiwe C, Zentner J, Volk B, Romstock J, Stefan H, Hildebrandt M. A new clinico-pathological classification system for mesial temporal sclerosis. *Acta Neuropathol* 2007; **113**: 235–44
31 de Lanerolle NC, Kim JH, Williamson A, Spencer SS, Zaveri HP, Eid T, Spencer DD. A retrospective analysis of hippocampal pathology in human temporal lobe epilepsy: evidence for distinctive patient subcategories. *Epilepsia* 2003; **44**: 677–87
32 Gaitatzis A, Sisodiya SM, Sander JW. The somatic comorbidity of epilepsy: a weighty but often unrecognized burden. *Epilepsia* 2012; **53**: 1282–93
33 Pandis D, Scarmeas N. Seizures in Alzheimer disease: clinical and epidemiological data. *Epilepsy Curr* 2012; **12**: 184–7
34 Greenfield JG, Love S, Louis DN, Ellison D. *Greenfield's Neuropathology*, 8th edn. London: Hodder Arnold, 2008
35 Chan-Palay V, Lang W, Haesler U, Kohler C, Yasargil G. Distribution of altered hippocampal neurons and axons immunoreactive with antisera against neuropeptide Y in Alzheimer's-type dementia. *J Comp Neurol* 1986; **248**: 376–94
36 Palop JJ, Chin J, Roberson ED, Wang J, Thwin MT, Bien-Ly N, Yoo J, Ho KO, Yu GQ, Kreitzer A, Finkbeiner S, Noebels JL, Mucke L. Aberrant excitatory neuronal activity and compensatory remodeling of inhibitory hippocampal circuits in mouse models of Alzheimer's disease. *Neuron* 2007; **55**: 697–711
37 Dumas TC, Powers EC, Tarapore PE, Sapolsky RM. Overexpression of calbindin D(28k) in dentate gyrus granule cells alters mossy fiber presynaptic function and impairs hippocampal-dependent memory. *Hippocampus* 2004; **14**: 701–9
38 Jouvenceau A, Potier B, Poindessous-Jazat F, Dutar P, Slama A, Epelbaum J, Billard JM. Decrease in calbindin content significantly alters LTP but not NMDA receptor and calcium channel properties. *Neuropharmacology* 2002; **42**: 444–58
39 Odero GL, Oikawa K, Glazner KA, Schapansky J, Grossman D, Thiessen JD, Motnenko A, Ge N, Martin M, Glazner GW, Albensi BC. Evidence for the involvement of calbindin D28k in the presenilin 1 model of Alzheimer's disease. *Neuroscience* 2010; **169**: 532–43
40 Palop JJ, Jones B, Kekonius L, Chin J, Yu GQ, Raber J, Masliah E, Mucke L. Neuronal depletion of calcium-dependent proteins in the dentate gyrus is tightly linked to Alzheimer's disease-related cognitive deficits. *Proc Natl Acad Sci USA* 2003; **100**: 9572–7
41 Moreno H, Burghardt NS, Vela-Duarte D, Masciotti J, Hua F, Fenton AA, Schwaller B, Small SA. The absence of the calcium-buffering protein calbindin is associated with faster age-related decline in hippocampal metabolism. *Hippocampus* 2012; **22**: 1107–20
42 Bouilleret V, Schwaller B, Schurmans S, Celio MR, Fritschy JM. Neurodegenerative and morphogenic changes in a mouse model of temporal lobe epilepsy do not depend on the expression of the calcium-binding proteins parvalbumin, calbindin, or calretinin. *Neuroscience* 2000; **97**: 47–58
43 Popovic M, Caballero-Bleda M, Kadish I, Van Groen T. Subfield and layer-specific depletion in calbindin-D28K, calretinin and parvalbumin immunoreactivity in the dentate gyrus of amyloid precursor protein/presenilin 1 transgenic mice. *Neuroscience* 2008; **155**: 182–91
44 Takahashi H, Brasnjevic I, Rutten BP, Van Der Kolk N, Perl DP, Bouras C, Steinbusch HW, Schmitz C, Hof PR, Dickstein DL. Hippocampal interneuron loss in an APP/PS1 double mutant mouse and in Alzheimer's disease. *Brain Struct Funct* 2010; **214**: 145–60
45 Ferrer I. Neurons and their dendrites in frontotemporal dementia. *Dement Geriatr Cogn Disord* 1999; **10** (Suppl. 1): 55–60
46 Corrada MM, Berlau DJ, Kawas CH. A population-based clinicopathological study in the oldest-old: the 90+ study. *Curr Alzheimer Res* 2012; **9**: 709–17

47 Pao WC, Dickson DW, Crook JE, Finch NA, Rademakers R, Graff-Radford NR. Hippocampal sclerosis in the elderly: genetic and pathologic findings, some mimicking Alzheimer disease clinically. *Alzheimer Dis Assoc Disord* 2011; **25**: 364–8
48 Peterson C, Kress Y, Vallee R, Goldman JE. High molecular weight microtubule-associated proteins bind to actin lattices (Hirano bodies). *Acta Neuropathol* 1988; **77**: 168–74
49 Myre MA. Clues to gamma-secretase, huntingtin and Hirano body normal function using the model organism Dictyostelium discoideum. *J Biomed Sci* 2012; **19**: 41
50 Shao CY, Mirra SS, Sait HB, Sacktor TC, Sigurdsson EM. Postsynaptic degeneration as revealed by PSD-95 reduction occurs after advanced Abeta and tau pathology in transgenic mouse models of Alzheimer's disease. *Acta Neuropathol* 2011; **122**: 285–92
51 Somogyi P, Klausberger T. Defined types of cortical interneurone structure space and spike timing in the hippocampus. *J Physiol* 2005; **562**: 9–26
52 Maccaferri G. Stratum oriens horizontal interneurone diversity and hippocampal network dynamics. *J Physiol* 2005; **562**: 73–80
53 Szilagyi T, Orban-Kis K, Horvath E, Metz J, Pap Z, Pavai Z. Morphological identification of neuron types in the rat hippocampus. *Rom J Morphol Embryol* 2011; **52**: 15–20
54 Decressac M, Barker RA. Neuropeptide Y and its role in CNS disease and repair. *Exp Neurol* 2012; **238**: 265–72
55 Ramos B, Baglietto-Vargas D, del Rio JC, Moreno-Gonzalez I, Santa-Maria C, Jimenez S, Caballero C, Lopez-Tellez JF, Khan ZU, Ruano D, Gutierrez A, Vitorica J. Early neuropathology of somatostatin/NPY GABAergic cells in the hippocampus of a PS1xAPP transgenic model of Alzheimer's disease. *Neurobiol Aging* 2006; **27**: 1658–72
56 Long L, Xiao B, Feng L, Yi F, Li G, Li S, Mutasem MA, Chen S, Bi F, Li Y. Selective loss and axonal sprouting of GABAergic interneurons in the sclerotic hippocampus induced by LiCl-pilocarpine. *Int J Neurosci* 2011; **121**: 69–85
57 Aronica E, Dickson DW, Kress Y, Morrison JH, Zukin RS. Non-plaque dystrophic dendrites in Alzheimer hippocampus: a new pathological structure revealed by glutamate receptor immunocytochemistry. *Neuroscience* 1998; **82**: 979–91
58 Furgerson M, Fechheimer M, Furukawa R. Model Hirano bodies protect against tau-independent and tau-dependent cell death initiated by the amyloid precursor protein intracellular domain. *Plos ONE* 2012; **7**: e44996
59 King A, Sweeney F, Bodi I, Troakes C, Maekawa S, Al-Sarraj S. Abnormal TDP-43 expression is identified in the neocortex in cases of dementia pugilistica, but is mainly confined to the limbic system when identified in high and moderate stages of Alzheimer's disease. *Neuropathology* 2010; **30**: 408–19
60 Kauffman MA, Consalvo D, Moron DG, Lereis VP, Kochen S. ApoE epsilon4 genotype and the age at onset of temporal lobe epilepsy: a case-control study and meta-analysis. *Epilepsy Res* 2010; **90**: 234–9
61 Yeni SN, Ozkara C, Buyru N, Baykara O, Hanoglu L, Karaagac N, Ozyurt E, Uzan M. Association between APOE polymorphisms and mesial temporal lobe epilepsy with hippocampal sclerosis. *Eur J Neurol* 2005; **12**: 103–7

Supporting information

Additional Supporting Information may be found in the online version of this article at the publisher's web-site:

Table S1. Clinical and pathology data of individual cases.

Received 12 April 2013
Accepted after revision 4 September 2013
Published online Article Accepted on 12 September 2013